

Calibrating multi-dimensional complex ODE from noisy data via deep neural networks

Kexuan Li

Department of Mathematical Sciences, Worcester Polytechnic Institute

Fangfang Wang

Department of Mathematical Sciences, Worcester Polytechnic Institute

Ruiqi Liu

Department of Mathematics and Statistics, Texas Tech University

Fan Yang

Eli Lilly and Company

Zuofeng Shang

Department of Mathematical Sciences, New Jersey Institute of Technology

April 18, 2021

Abstract

Ordinary differential equations (ODEs) are widely used to model complex dynamics that arises in biology, chemistry, engineering, finance, physics, etc. Calibration of a complicated ODE system using noisy data is generally very difficult. In this work, we propose a two-stage nonparametric approach to address this problem. We first extract the de-noised data and their higher order derivatives using boundary kernel method, and then feed them into a sparsely connected deep neural network with ReLU activation function. Our method is able to recover the ODE system without being subject to the curse of dimensionality and complicated ODE structure. When the ODE possesses a general modular structure, with each modular component involving only a few input variables, and the network architecture is properly chosen, our method is proven to be consistent. Theoretical properties are corroborated by an extensive simulation study that demonstrates the validity and effectiveness of the proposed method. Finally, we use our method to simultaneously characterize the growth rate of Covid-19 infection cases from 50 states of the USA.

Keywords: Boundary kernel function; Sparsely connected deep neural networks; Nonlinear ODE in high dimensions; ReLu activation function.

1 Introduction

The use of ordinary differential equations (ODEs) is prevalent in both social and natural sciences to study complex dynamic phenomena or dynamical systems. For instance, linear ODEs are often used to describe population growth ([Henderson and Loreau, 2019]), Lorenz equation—a high-dimensional nonlinear ODE—used to characterize chaos systems ([Talwar and Namachchivaya Sri, 1992]), and high-dimensional linear ODEs used to construct a dynamic gene regulatory network ([Lu et al., 2011]). Therefore, calibrating complicated ODE systems is of great interest and importance to both theorists and practitioners.

Owing to the superior performance of deep learning in modeling complicated data, deep neural networks have been actively used to reproduce dynamical systems ([Weinan, 2017]). Deep neural networks, such as residual network ([He et al., 2016]) and discrete normalizing flows ([Kobyzev et al., 2020]), can be considered as discrete dynamical systems. Recently, [Chen et al., 2018] propose a new family of continuous neural networks that extend the traditional discrete sequence of hidden layers to continuous-depth by using an ODE to parameterize the hidden units. [Lusch et al., 2018] and [Champion et al., 2019] consider autoencoder-based architecture to understand and predict the complex dynamical systems.

Despite advances in deep learning, most of the existing methods lack interpretability and their theoretical underpinnings are not well grounded. In this paper, we attempt to fill the gap and provide statistical justification for calibrating a complex system which can be characterized by multi-dimensional nonlinear ODEs. In particular, we are interested in scenarios where data, collected from continuous-time nonlinear ODEs, are asynchronous, irregularly spaced and are contaminated by measurement errors.

To start with, consider the following general multi-dimensional ν th order ODE system:

$$\frac{d^\nu}{dt^\nu} \mathbf{x}(t) = \mathbf{f}_0(\mathbf{x}(t), \mathbf{x}^{(1)}(t), \dots, \mathbf{x}^{(\nu-1)}(t)), \quad 0 \leq t \leq 1, \quad (1)$$

where $\mathbf{x}(t) = (x_1(t), \dots, x_d(t))^\top \in \mathbb{R}^d$ is a d -dimensional function of t , $\mathbf{x}^{(j)}(t)$ represents the j th derivative of $\mathbf{x}(t)$, and $\mathbf{f}_0(\cdot) = (f_{0,1}(\cdot), \dots, f_{0,d}(\cdot))^\top : \mathbb{R}^{r_0} \rightarrow \mathbb{R}^d$ is the ground-truth but unknown, with $r_0 = \nu d$. When $\nu = 1$, (1) degenerates to a first-order ODE system:

$$\frac{d\mathbf{x}(t)}{dt} = \mathbf{f}_0(\mathbf{x}(t)), \quad 0 \leq t \leq 1. \quad (2)$$

In general, \mathbf{f}_0 often implies unknown interactions among $\mathbf{x}(t), \mathbf{x}^{(1)}(t), \dots$, and $\mathbf{x}^{(\nu-1)}(t)$, which is computationally difficult using conventional nonparametric techniques. Meanwhile, in many applications, it is impossible to observe $\mathbf{x}(t)$ directly. Instead, we observe y_{ji} which satisfy

$$y_{ji} = x_j(t_{ji}) + \epsilon_{ji}, \quad i = 1, \dots, n_j, \quad (3)$$

at discrete time points $0 \leq t_{j1} < t_{j2} < \dots < t_{jn_j} \leq 1$ for each component j , $j = 1, \dots, d$, where $\epsilon_{ji} \sim N(0, \sigma_j^2)$ represents the measurement error at time t_{ji} . The data observed for each

component are allowed to be from different time stamps which might not be equally spaced, thereby, yielding different sample sizes n_j for different components. The statistical task is to estimate the multi-dimensional nonlinear function \mathbf{f}_0 in (1) using the observed noisy data $\mathbf{y}_1, \dots, \mathbf{y}_d$, where $\mathbf{y}_j = (y_{j1}, \dots, y_{jn_j})^\top$. To achieve this, we propose a two-stage procedure for estimating \mathbf{f}_0 nonparametrically. In Stage 1, we use kernel estimation to filter out the noisy in $\{\mathbf{y}_1, \dots, \mathbf{y}_d\}$ and obtain $\hat{\mathbf{x}}(t)$ and its high order derivative $\hat{\mathbf{x}}^{(j)}(t)$, $j = 1, 2, \dots, \nu$, which will be shown to be consistent for $\mathbf{x}(t)$ and $\hat{\mathbf{x}}^{(j)}(t)$, respectively (see Section 3.1). In Stage 2, we adopt a ReLU feedforward neural network to approximate $\hat{\mathbf{x}}^{(\nu)}(t)$ (See Section 3.2). By assuming that the function $\mathbf{f}_0(\cdot)$ enjoys a general modular structure with each modular component involving only a few input variables, we establish the consistency of the ReLU feedforward neural network estimator and derive its convergence rate. In particular, we prove that the rate is not subject to the dimension of ODE system, but depends solely on the length and width of the neural network $\hat{\mathbf{f}}(\cdot)$ and the smoothness of the function $\mathbf{f}_0(\cdot)$. As such, our method is computationally more tractable than conventional nonparametric methods.

Terminologies and Notation: In this paper all vectors are column vectors. Let $\|\mathbf{v}\|_2^2 = \mathbf{v}^\top \mathbf{v}$ for any vector \mathbf{v} . Let $\|f\|_2^2 = \int f(x)^2 dx$ be the L_2 norm of a real-valued function $f(x)$. For two positive sequences a_n and b_n , we say $a_n \lesssim b_n$ if there exists a positive constant c such that $a_n \leq cb_n$ for all n , and $a_n \asymp b_n$ if $c^{-1}a_n \leq b_n \leq ca_n$ for some constant $c > 1$ and a sufficiently large n . Suppose $\mathbf{x} = (x_1, \dots, x_d)^\top$ is a d -dimensional vector. Let $|\mathbf{x}| = (|x_1|, \dots, |x_d|)^\top$ denote the absolute value of \mathbf{x} , $|\mathbf{x}|_\infty = \max_{i=1, \dots, d} |x_i|$, $|\mathbf{x}|_0 = \sum_{i=1}^d \mathbb{1}(x_i \neq 0)$. For two d -dimensional vectors \mathbf{x}, \mathbf{y} , we say $\mathbf{x} \lesssim \mathbf{y}$ if $x_i \lesssim y_i$, for $i = 1, \dots, d$. Let $\lfloor x \rfloor$ be the largest integer less than x and $\lceil x \rceil$ be the smallest integer greater than x . Let $\|A\|_\infty = \max_{ij} |a_{ij}|$ be the max norm and $\|A\|_0$ be the number of non-zero entries of a matrix $A = (a_{ij})$, and $\|\mathbf{f}\|_\infty\|_\infty$ be the sup-norm for a d -dimensional function \mathbf{f} . We use $a \wedge b$ and $a \vee b$ to represent the minimum and maximum of two numbers, respectively.

2 Related work

In a parametric/semi-parametric setting where $\mathbf{f}_0(\cdot)$ is parameterized, the process of calibrating the unknown parameters is the so-called inverse problem and has been widely studied in the statistical literature. For example, if $n_1 = n_2 = \dots = n_d = n$, $t_{1i} = t_{2i} = \dots = t_{di}$, for $i = 1, \dots, n$, and suppose that (2) involves an unknown parameter θ , i.e., $\frac{d\mathbf{x}(t; \theta)}{dt} = \mathbf{f}_0(\mathbf{x}(t; \theta); \theta)$, then θ can be estimated by the least square estimator (e.g., see [Benson, 1979], [Biegler et al., 1986]):

$$\hat{\theta}_{LSE} = \underset{\theta}{\operatorname{argmin}} \sum_{i=1}^n \sum_{j=1}^d (y_{ji} - x_j(t_{ji}))^2, \quad \text{subject to } \frac{d\mathbf{x}(t; \theta)}{dt} = \mathbf{f}_0(\mathbf{x}(t; \theta); \theta).$$

If the measurement errors ϵ_{ji} are normally distributed, then $\hat{\theta}_{LSE}$ coincides with the maximum likelihood estimator and is \sqrt{n} -consistent. In most cases, $\hat{\theta}_{LSE}$ has no closed-form expression and the least square estimation tends to be computationally expensive. To overcome this problem, many other methods have been developed; see [Liang and Wu, 2008], [Hall and Ma, 2014], [Bhaumik and Ghosal, 2015], [Wu et al., 2019], [Sun et al., 2020], among

many others. Nonetheless, they suffer from the curse of dimensionality and can only deal with lower order derivatives.

In the cases where \mathbf{f}_0 can not be summarized by a few low-dimensional parameters, calibrating \mathbf{f}_0 becomes more demanding. Existing solutions attempt to impose extra assumptions so as to simplify the structure of \mathbf{f}_0 . For instance, [Henderson and Michailidis, 2014] and [Chen et al., 2017] assume an additive structure on \mathbf{f}_0 , while [Paul et al., 2016] consider a case where \mathbf{f}_0 is positive. To well preserve the structure of \mathbf{f}_0 so as to align with what is observed in practice, we suggest a two-stage deep learning method that estimates \mathbf{f}_0 nonparametrically by imposing a general modular structure on \mathbf{f}_0 with each modular component involving only a few input variables. This method can deal with higher order derivatives and is able to recover the ODE system without being subject to the curse of dimensionality.

Recently, deep neural network has been successfully applied in many fields, such as computer vision, natural language processing, bioinformatics, recommendation systems, etc. Investigating theoretical properties of deep neural network have also attracted many researchers' interests. In the statistical literature, [Schmidt-Hieber, 2020] proves that using sparsely connected deep neural networks with ReLU activation function can achieve the minimax rate of convergence in a nonparametric setting. [Farrell et al., 2021] achieve similar convergence rates as [Schmidt-Hieber, 2020] under different regularity conditions. Similarly, [Bauer and Kohler, 2019] show that multilayer feed-forward neural networks are able to circumvent the curse of dimensionality if the regression function satisfies a generalized hierarchical interaction model. Another point of view to theoretically understanding deep learning is from approximation theory; e.g., see [Elbrächter et al., 2021], [Lu et al., 2020], [Hammer, 2000], [Li et al., 2020], [Li et al., 2019]. Unlike the traditional function approximation theory that uses the aggregation of simple functions to approximate complicated ones, deep neural networks use the compositions of simple functions, which motivates us to assume the underlining function \mathbf{f}_0 satisfies a compositional structure.

3 Methodology and Main Theorem

In this section, we detail the two-stage estimation procedure and provide its theoretical underpinnings.

3.1 Stage 1: Kernel Estimator

Our goal in the first stage is to estimate $\mathbf{x}(t) = (x_1(t), \dots, x_d(t))^\top$ and its ν th derivative $\mathbf{x}^{(\nu)}(t)$, $\nu \geq 1$, on the basis of the “noisy” observations $\{\mathbf{y}_1, \dots, \mathbf{y}_d\}$. This is achieved via kernel estimation by casting (3) as a nonparametric regression.

The classical kernel estimator of $x_j(t)$, $j = 1, \dots, d$, is given by

$$\tilde{x}_j(t) = \sum_{i=1}^{n_j} \frac{t_{ji} - t_{j(i-1)}}{h} K\left(\frac{t - t_{ji}}{h}\right) \cdot y_j(t_{ji}),$$

where $t_{j0} = 0$ and h is a sequence of positive bandwidths satisfying $h \rightarrow 0$ and $n_j h \rightarrow \infty$ as

$n_j \rightarrow \infty$, and where $K(\cdot)$ is a non-negative kernel function satisfying

$$\int_{-\infty}^{\infty} K(x)dx = 1, \quad \int_{-\infty}^{\infty} (K(x))^2 dx < \infty, \quad \text{and } K(x) \text{ is Lipschitz continuous.} \quad (4)$$

Despite that $\tilde{x}_j(t)$ is consistent for $x_j(t)$ for $t \in (0, 1)$ (see [Priestley and Chao, 1972]), it does not lead to a consistent estimator of $x_j^{(\nu)}(t)$. Therefore, we adopt the boundary kernel function introduced in [Gasser and Müller, 1984] here. We first estimate $x_j(t), j = 1, \dots, d$, by

$$\hat{x}_j(t) = \frac{1}{h} \sum_{i=1}^{n_j} \int_{s_{i-1}}^{s_i} K\left(\frac{t-u}{h}\right) du \cdot y_j(t_{ji}), \quad (5)$$

where $0 = s_0 \leq s_1, \dots, \leq s_{n_j} = 1$, $s_i \in [t_{ji}, t_{j(i+1)}]$, $i = 1, \dots, n_j - 1$, h is a sequence of positive bandwidths satisfying $h \rightarrow 0$ and $n_j h \rightarrow \infty$ as $n_j \rightarrow \infty$, and where $K(\cdot)$ is a ν times differentiable kernel function that has a compact support on $[-\tau, \tau]$ with $K(-\tau) = K(\tau) = 0$ and fulfills (4) and its ν th derivative, K_ν , meets the following requirements:

- (i) The support of K_ν is $[-\tau, \tau]$ and $\int_{-\tau}^{\tau} K_\nu(x)dx = 1$;
- (ii) For constants $\beta \in \mathbb{R}$ and $k \geq \nu + 2$,

$$\int_{-\tau}^{\tau} K_\nu(x)x^j dx = \begin{cases} 0 & j = 0, \dots, \nu - 1, \nu + 1, \dots, k - 1, \\ (-1)^\nu \nu!, & j = \nu, \\ \beta, & j = k. \end{cases} \quad (6)$$

In order to obtain a consistent estimator of $\mathbf{x}^{(\nu)}(t)$ for $t \in [0, 1]$, i.e., to eliminate boundary effects which become prominent when estimating derivatives, we introduce the modified kernel $K_{\nu,q}$ with support $[-\tau, q\tau]$, for some $q \in [0, 1]$, satisfying $K_{\nu,q} \rightarrow K_\nu$ as $q \rightarrow 1$. Moreover, $K_{\nu,q}(x)$ satisfies (6) with a uniformly bounded k -th moment for q , and the asymptotic variance of $K_{\nu,q}$ is bounded uniformly for q ([Gasser and Müller, 1984]). Therefore, $x_j^{(\kappa)}(t)$ is estimated by

$$\hat{x}_j^{(\kappa)}(t) = \frac{1}{h^{\kappa+1}} \sum_{i=1}^{n_j} \int_{s_{i-1}}^{s_i} K_{\kappa,q}\left(\frac{t-u}{h}\right) du \cdot y_j(t_{ji}), \quad \text{for } \kappa = 1, \dots, \nu. \quad (7)$$

[Gasser and Müller, 1984] and [Gasser et al., 1985] have discussed the existence of such kernel functions $K(\cdot)$ and $K_{\nu,q}(x)$, and proved that if the sequence $\{s_i\}$ satisfies $\max_i |s_i - s_{i-1} - n^{-1}| = O(n^{-\delta})$ for some $\delta > 1$, then $\int_0^1 \|\hat{\mathbf{x}}^{(\nu)}(t) - \mathbf{f}_0(\mathbf{x}(t), \mathbf{x}^{(1)}(t), \dots, \mathbf{x}^{(\nu-1)}(t))\|_2^2 dt = O_P(n^{-2(k-\nu)/(2k+1)})$.

3.2 Stage 2: Deep Neural Network Estimator

In Stage 2, we use a multilayer feedforward neural network to approximate the unknown ground-truth $\mathbf{f}_0(\cdot)$. We start off by introducing the definitions of Hölder smoothness and compositional functions.

Definition 1. A function $g : \mathbb{R}^{r_0} \rightarrow \mathbb{R}$ is said to be (β, C) -Hölder smooth for some positive constants β and C , if for every $\gamma = (\gamma_1, \dots, \gamma_{r_0})^\top \in \mathbb{N}^{r_0}$ the following two conditions hold:

$$\sup_{\mathbf{z} \in \mathbb{R}^{r_0}} \left| \frac{\partial^\kappa g}{\partial z_1^{\gamma_1} \dots \partial z_{r_0}^{\gamma_{r_0}}}(\mathbf{z}) \right| \leq C, \quad \text{for } \kappa \leq \lfloor \beta \rfloor,$$

and

$$\left| \frac{\partial^\kappa g}{\partial z_1^{\gamma_1} \dots \partial z_{r_0}^{\gamma_{r_0}}}(\mathbf{z}) - \frac{\partial^\kappa g}{\partial z_1^{\gamma_1} \dots \partial z_{r_0}^{\gamma_{r_0}}}(\tilde{\mathbf{z}}) \right| \leq C \|\mathbf{z} - \tilde{\mathbf{z}}\|_2^{\beta - \lfloor \beta \rfloor}, \quad \text{for } \kappa = \lfloor \beta \rfloor \text{ and } \mathbf{z}, \tilde{\mathbf{z}} \in \mathbb{R}^{r_0},$$

where $\kappa = \sum_{i=1}^{r_0} \gamma_i$.

For convenience, we say g is (∞, C) -Hölder smooth if g is (β, C) -Hölder smooth for all $\beta > 0$. Hölder smoothness is commonly assumed for estimating regression functions in the literature on nonparametric function estimation (see, for instance, [Stone, 1985] and [Ferraty and Vieu, 2006]).

Definition 2. A function $f : \mathbb{R}^{r_0} \rightarrow \mathbb{R}$ is said to have a compositional structure with parameters $(L_*, \mathbf{r}, \tilde{\mathbf{r}}, \boldsymbol{\beta}, \mathbf{a}, \mathbf{b}, \mathbf{C})$ for $L_* \in \mathbb{Z}_+$, $\mathbf{r} = (r_0, \dots, r_{L_*+1})^\top \in \mathbb{Z}_+^{L_*+2}$, with $r_{L_*+1} = 1$, $\tilde{\mathbf{r}} = (\tilde{r}_0, \dots, \tilde{r}_{L_*})^\top \in \mathbb{Z}_+^{L_*+1}$, $\boldsymbol{\beta} = (\beta_0, \dots, \beta_{L_*})^\top \in \mathbb{R}_+^{L_*+1}$, $\mathbf{a} = (a_0, \dots, a_{L_*+1})^\top$, $\mathbf{b} = (b_0, \dots, b_{L_*+1})^\top \in \mathbb{R}^{L_*+2}$, and $\mathbf{C} = (C_0, \dots, C_{L_*})^\top \in \mathbb{R}_+^{L_*+1}$, if

$$f(\mathbf{z}) = \mathbf{g}_{L_*} \circ \dots \circ \mathbf{g}_1 \circ \mathbf{g}_0(\mathbf{z}), \quad \mathbf{z} \in [a_0, b_0]^{r_0}$$

where $\mathbf{g}_i = (g_{i,1}, \dots, g_{i,r_{i+1}})^\top : [a_i, b_i]^{r_i} \rightarrow [a_{i+1}, b_{i+1}]^{r_{i+1}}$ for some $|a_i|, |b_i| \leq C_i$, and the functions $g_{i,j} : [a_i, b_i]^{r_i} \rightarrow [a_{i+1}, b_{i+1}]$ are (β_i, C_i) -Hölder smooth only relying on \tilde{r}_i variables.

Without loss of generality, we can always assume $C_i > 1$, $i = 1, \dots, L_*$. Denote by $\mathcal{CS}(L_*, \mathbf{r}, \tilde{\mathbf{r}}, \boldsymbol{\beta}, \mathbf{a}, \mathbf{b}, \mathbf{C})$ the class of compositional functions defined above. It is pointed out by, for instance, [Schmidt-Hieber, 2020] that a compositional function can be approximated by a neural network with any order of accuracy. Due to its popularity, it is also adopted by [Bauer and Kohler, 2019], [Schmidt-Hieber, 2020], [Kohler and Langer, 2019], [Liu et al., 2020], [Liu et al., 2019], [Wang et al., 2020] to study nonparametric regression problems.

By Definition 2, any function in $\mathcal{CS}(L_*, \mathbf{r}, \tilde{\mathbf{r}}, \boldsymbol{\beta}, \mathbf{a}, \mathbf{b}, \mathbf{C})$ is composed of L_* layers, and in the i -th layer, $i = 0, \dots, L_*$, there are only \tilde{r}_i "active" variables. This implicitly assumes a sparsity structure in each layer, which prevents us from the curse of dimensionality. The intuition behind this definition comes from the structure of feedforward neural network (see Definition 4). Clearly, a feedforward neural network belongs to $\mathcal{CS}(L_*, \mathbf{r}, \tilde{\mathbf{r}}, \boldsymbol{\beta}, \mathbf{a}, \mathbf{b}, \mathbf{C})$, with the i -th hidden layer in the network viewed as \mathbf{g}_i .

In Definition 2, functions in each layer $g_{i,j} : [a_i, b_i]^{r_i} \rightarrow [a_{i+1}, b_{i+1}]$ are (β_i, C_i) -Hölder smooth and it is not difficult to verify that the composed function f is also Hölder smooth. To proceed, we need to introduce the following two definitions which capture the intrinsic smoothness and dimension of the compositional functions.

Definition 3 (Intrinsic Smoothness and Intrinsic Dimension). For $f \in \mathcal{CS}(L_*, \mathbf{r}, \tilde{\mathbf{r}}, \boldsymbol{\beta}, \mathbf{a}, \mathbf{b}, \mathbf{C})$, the intrinsic smoothness and intrinsic dimension of f are defined as:

$$\beta^* = \beta_{i^*}^* \quad \text{and} \quad r^* = \tilde{r}_{i^*},$$

respectively, where $\beta_i^* = \beta_i \prod_{s=i+1}^{L_*} (\beta_s \wedge 1)$ for $i = 0, \dots, L_*$, and $i^* = \operatorname{argmin}_{0 \leq i \leq L_*} \beta_i^*/\tilde{r}_i$. We will adopt the convention $\prod_{s=L_*+1}^{L_*} (\beta_s \wedge 1) = 1$ for convenience.

It is worth noting that the order of Hölder smoothness of a function f is less than its intrinsic smoothness. Throughout the paper, we assume the true functions $f_{0,j} \in \mathcal{CS}(L_*, \mathbf{r}, \tilde{\mathbf{r}}, \boldsymbol{\beta}, \mathbf{a}, \mathbf{b}, \mathbf{C})$, $j = 1, \dots, d$. This assumption is not restrictive, as the compositional structure covers a wide collection of functions. Here are some examples.

Example 1. (Homogeneous Linear ODE system) Consider the following dynamical system

$$\frac{d^\nu}{dt^\nu} \begin{bmatrix} x_1(t) \\ \vdots \\ x_d(t) \end{bmatrix} = \begin{bmatrix} a_{1,1} & \dots & a_{1,\nu d} \\ \vdots & \ddots & \vdots \\ a_{d,1} & \dots & a_{d,\nu d} \end{bmatrix} \begin{bmatrix} x_1(t) \\ \vdots \\ x_d^{(\nu-1)}(t) \end{bmatrix}.$$

In this example, each component $x_j^{(\nu)}$ has a compositional structure with $L_* = 0$, $\mathbf{r} = (\nu d, 1)^\top$, $\tilde{\mathbf{r}} = \nu d$, $\boldsymbol{\beta} = \infty$. Therefore, $\beta^* = \infty$ and $r^* = \nu d$.

Example 2. (Additive Model) Consider a more general case than Example 1. Define $x_i^{(\nu)} = g_i(\sum_{j=1}^d \sum_{k=0}^{\nu-1} f_{j,k}(x_j^{(k)}))$, where $g_i(\cdot)$ is (β_g, C_g) -Hölder smooth and $f_{j,k}(\cdot)$ is (β_f, C_f) -Hölder smooth. Clearly, $x_i^{(\nu)}$ can be written as a composition of three functions $x_i^{(\nu)} = h_2 \circ h_1 \circ h_0$ with $h_0(x_1, \dots, x_d^{(\nu-1)}) = (f_{1,0}(x_1), \dots, f_{d,\nu-1}(x_d^{(\nu-1)}))$, $h_1(x_1, \dots, x_{\nu d}) = \sum_{i=1}^{\nu d} x_i$, and $h_2(x) = g_i(x)$. Here $L_* = 2$, $\mathbf{r} = (\nu d, \nu d, 1, 1)$, $\tilde{\mathbf{r}} = (1, \nu d, 1)$, $\boldsymbol{\beta} = (\beta_h, \infty, \beta_g)$, $\beta^* = \min(\beta_h, \beta_g)$, and $r^* = 1$.

For $\mathbf{v} = (v_1, \dots, v_r)^\top \in \mathbb{R}^r$, define the shifted activation function $\sigma_{\mathbf{v}}(\mathbf{x}) = (\sigma(x_1 - v_1), \dots, \sigma(x_r - v_r))^\top$, where $\sigma(s) := \max\{0, s\}$ and $\mathbf{x} = (x_1, \dots, x_r) \in \mathbb{R}^r$. We next introduce the ReLU Feedforward Neural Network which is widely used in the deep learning literature.

Definition 4 (ReLU Feedforward Neural Network). A ReLU feedforward neural network $\mathbf{f}(\mathbf{x}; W, v)$ is defined as

$$\mathbf{f}(\mathbf{x}; W, v) := W_L \sigma_{\mathbf{v}_L} \dots W_1 \sigma_{\mathbf{v}_1} W_0 \mathbf{x}, \quad \mathbf{x} \in \mathbb{R}^{p_0}, \quad (8)$$

where $W \in \mathcal{W} := \{(W_0, \dots, W_L) : W_l \in \mathbb{R}^{p_{l+1} \times p_l}, 0 \leq l \leq L\}$ is the weight matrix, $v \in \mathcal{V} := \{(\mathbf{v}_1, \dots, \mathbf{v}_L) : \mathbf{v}_l \in \mathbb{R}^{p_l}, 1 \leq l \leq L\}$ is the bias term, and $\sigma_{\mathbf{v}}$ is the shifted activation function, and p_0, \dots, p_{L+1} are positive integers.

In Definition 4, L is the number of hidden layers and the width vector $\mathbf{p} = (p_0, \dots, p_{L+1})$ specifies the number of units in each layer, i.e., the width of the network. The ReLU feedforward neural network is parameterized by $(W_j)_{j=0, \dots, L}$ and $(\mathbf{v}_j)_{j=1, \dots, L}$.

In this paper, we consider two subclasses of ReLU Feedforward neural networks:

$$\mathcal{F}_1(L, \mathbf{p}) := \{\mathbf{f}(\mathbf{x}; W, v) \text{ of form (8)} : \max_{j=0, \dots, L} \|W_j\|_\infty + |\mathbf{v}_j|_\infty \leq 1\}, \quad (9)$$

where \mathbf{v}_0 is a vector of zeros, and

$$\mathcal{F}_2(L, \mathbf{p}, \tau, F) := \{\mathbf{f}(\mathbf{x}; W, v) \in \mathcal{F}_1(L, \mathbf{p}) : \sum_{j=0}^L (\|W_j\|_0 + |\mathbf{v}_j|_0) \leq \tau, \|\mathbf{f}\|_\infty \leq F\}. \quad (10)$$

The subclass (9) comprises the fully connected networks with bounded parameters, and it is not empty in that we can always divide all the weights by the maximum weight. In practice, people tend to use dropout as a regularization technique to prevent overfitting, i.e., randomly setting parts of neurons to zero. So it is natural to consider a sparse neural network as specified in (10). The two subclasses of neural networks are also employed in [Schmidt-Hieber, 2020] and [Wang et al., 2020] to nonparametrically estimate regression function based on i.i.d. data and functional data.

Next we present the estimator of $\mathbf{f}_0(\cdot)$ in (1) via a sparsely connected deep neural network. Let $\widehat{\mathbf{x}}(t) = (\widehat{x}_1(t), \dots, \widehat{x}_d(t))^\top$ and $\widehat{\mathbf{x}}^{(\nu)}(t) = (\widehat{x}_1^{(\nu)}(t), \dots, \widehat{x}_d^{(\nu)}(t))^\top$, where $\widehat{x}_j(t)$ and $\widehat{x}_j^{(\nu)}(t)$ are respectively from (5) and (7). The idea is to search for a member in $\mathcal{F}_2(L, \mathbf{p}, \tau, F)$ to well approximate $\mathbf{f}_0(\mathbf{x}(t), \mathbf{x}^{(1)}(t), \dots, \mathbf{x}^{(\nu-1)}(t))$. Specifically, the "best" estimator of $\mathbf{f}_0(\mathbf{x}(t), \dots, \mathbf{x}^{(\nu-1)}(t))$, or equivalently $\mathbf{x}^{(\nu)}(t)$, is obtained by minimizing

$$\int_0^1 \|\widehat{\mathbf{x}}^{(\nu)}(t) - \mathbf{f}(\widehat{\mathbf{x}}(t), \widehat{\mathbf{x}}^{(1)}(t), \dots, \widehat{\mathbf{x}}^{(\nu-1)}(t); W, v)\|_2^2 dt, \quad (11)$$

over all $\mathbf{f}(\mathbf{z}; W, v) \in \mathcal{F}_2(L, \mathbf{p}, \tau, F)$ with $\mathbf{p} = (r_0, p_1, \dots, p_L)$ and $\mathbf{z} \in \mathbb{R}^{r_0}$. The resulting estimator is denoted by $\widehat{\mathbf{f}}(\mathbf{z}; \widehat{W}, \widehat{v})$. The entire two-stage estimation procedure is summarized below:

Algorithm 1

- 1: **Input:** observed values $\{\mathbf{y}_1, \dots, \mathbf{y}_d\}$.
- 2: **for** each component j , $j = 1, \dots, d$ **do**
- 3: Estimate $x_j(t)$ and its higher order derivative $x_j^{(\kappa)}(t)$, $\kappa = 1, \dots, \nu$ through (5) and (7), respectively: $\widehat{x}_j(t) = \frac{1}{h} \sum_{i=1}^{n_j} \int_{s_{i-1}}^{s_i} K(\frac{t-u}{h}) du \cdot y_j(t_{ji})$ and $\widehat{x}_j^{(\kappa)}(t) = \frac{1}{h^{\kappa+1}} \sum_{i=1}^{n_j} \int_{s_{i-1}}^{s_i} K_{\kappa, q}(\frac{t-u}{h}) du \cdot y_j(t_{ji})$, for $\kappa = 1, \dots, \nu$
- 4: where the tuning parameter can be determined by cross validation.
- 5: **end for**
- 6: Use $(\widehat{\mathbf{x}}(t), \widehat{\mathbf{x}}^{(1)}(t), \dots, \widehat{\mathbf{x}}^{(\nu-1)}(t))$ as the input to fit $\widehat{\mathbf{x}}^{(\nu)}(t)$ through (11).
- 7: **Output:** $\widehat{\mathbf{f}}(\mathbf{z}; \widehat{W}, \widehat{v}) := \operatorname{argmin}_{\mathbf{f} \in \mathcal{F}_2(L, \mathbf{p}, \tau, F)} \int_0^1 \|\widehat{\mathbf{x}}^{(\nu)}(t) - \mathbf{f}(\widehat{\mathbf{x}}(t), \widehat{\mathbf{x}}^{(1)}(t), \dots, \widehat{\mathbf{x}}^{(\nu-1)}(t); W, v)\|_2^2 dt$

The following theorem establishes the consistency of $\widehat{\mathbf{f}}(\mathbf{z}; \widehat{W}, \widehat{v})$ as an estimator of $\mathbf{f}_0(\mathbf{x}(t), \dots, \mathbf{x}^{(\nu-1)}(t))$ and its convergence rate.

Theorem 1. *Suppose the true functions $f_{0,j} \in \mathcal{CS}(L_*, \mathbf{r}, \tilde{\mathbf{r}}, \boldsymbol{\beta}, \mathbf{a}, \mathbf{b}, C)$, $j = 1, \dots, d$. Consider the subclass $\mathcal{F}_2(L, \mathbf{p}, \tau, F)$. Further assume that $F \geq \max_{i=0, \dots, L^*} (C_i, 1)$, $N := \min_{i=1, \dots, L} p_i \geq 6\eta \max_{i=0, \dots, L_*} (\beta_i + 1)^{\tilde{r}_i} \vee (\tilde{C}_i + 1)e^{\tilde{r}_i}$ where $\eta = \max_{i=0, \dots, L_*} (r_{i+1}(\tilde{r}_i + \lceil \beta_i \rceil))$, and $\tau \lesssim LN$. Then we have*

$$\int_0^1 \|\widehat{\mathbf{f}}(\mathbf{x}(t), \dots, \mathbf{x}^{(\nu-1)}(t); \widehat{W}, \widehat{v}) - \mathbf{f}_0(\mathbf{x}(t), \dots, \mathbf{x}^{(\nu-1)}(t))\|_2^2 dt = O_P(\varsigma_n),$$

$$\int_0^1 \|\widehat{\mathbf{f}}(\widehat{\mathbf{x}}(t), \dots, \widehat{\mathbf{x}}^{(\nu-1)}(t); \widehat{W}, \widehat{v}) - \mathbf{f}_0(\mathbf{x}(t), \dots, \mathbf{x}^{(\nu-1)}(t))\|_2^2 dt = O_P(\varsigma_n),$$

where

$$\varsigma_n = (1 + N^L)n^{-2(k-\nu)/(2k+1)} + (N2^{-L})^2 \prod_{l=1}^{L^*} \beta_l \wedge 1 + N^{-\frac{2\beta^*}{r^*}} + \frac{LN \log(n) + L^2 N \log(LN)}{n},$$

β^* and r^* are the intrinsic smoothness and intrinsic dimension defined in Definition 3, and \tilde{C}_i 's are constants only depending on $\mathbf{C}, \mathbf{a}, \mathbf{b}$.

The consistency of $\hat{\mathbf{f}}(\mathbf{z}; \hat{W}, \hat{v})$ is guaranteed, if, for instance, $L \asymp (\log n)^{1/2}$ and $N \asymp e^{(\log n)^{1/4}}$, as the latter implies $\varsigma_n \rightarrow 0$ as $n \rightarrow \infty$.

4 Numerical experiments

In this section, we carry out extensive simulations to assess the performance of the proposed two-stage estimation procedure for two different designs of ODE systems.

4.1 Simulation Designs

In the first simulation (Design 1), we suppose that the true process is governed by the following linear ODE system: $\mathbf{x}^{(1)}(t) = A\mathbf{x}(t) + \mathbf{b}$, $0 \leq t \leq 1$, where A is a $d \times d$ sparse matrix and \mathbf{b} is a d -dimensional vector referred to as the initial value. Elements of \mathbf{b} are sampled from the uniform distribution $U(0, 1)$. We further define a set $J = \{j_1, j_2, j_3, j_4, j_5\}$, where j_k , $k = 1, \dots, 5$, are randomly sampled from $\{1, \dots, d\}$ without replacement. The sparse matrix $A = (a_{ij})$ is defined as, for $i = 1, \dots, d$,

$$a_{ij} \begin{cases} = 0 & j \notin J, \\ \sim U(0, 1) & j \in J. \end{cases}$$

In other words, each row of A has five non-zero values that are sampled from the uniform distribution. It is easy to verify $f_{0,j} \in \mathcal{CS}(L_*, \mathbf{r}, \tilde{\mathbf{r}}, \boldsymbol{\beta}, \mathbf{a}, \mathbf{b}, \mathbf{C})$, $j = 1, \dots, d$, with $L_* = 0$, $\mathbf{r} = (d, 1)^\top$, $\tilde{\mathbf{r}} = 5$, $\boldsymbol{\beta} = \infty$, $\beta^* = \infty$, and $r^* = 5$. For simplicity, we set $n_1 = n_2 = \dots = n_d = n$. The "observed" data are generated from $y_{ji} = x_j(t_i) + \epsilon_{ji}$, $i = 1, \dots, n$, $j = 1, \dots, d$, where $t_i = i/n$ and ϵ_{ji} are sampled from $N(0, 1)$. The sample size n and dimension d are chosen to be $n = 100, 200, 500$ and $d = 10, 100, 1000$.

In the second simulation (Design 2), we consider a second order nonlinear ODE system: $x_1^{(2)}(t) = 2\frac{x_1(t)}{x_3(t)} + 4x_4^{(1)}(t) - x_3(t)x_4(t)$, $x_2^{(2)}(t) = -x_4^{(1)}(t)$, $x_3^{(2)}(t) = 2$, $x_4^{(2)}(t) = x_2^{(1)}(t)$, $x_5^{(2)}(t) = x_5(t)$, $x_6^{(2)}(t) = -x_5^2(t)x_6(t) + x_6^{(1)}(t)$, $x_7^{(2)}(t) = x_7^{(1)}(t)x_2^{(1)}(t) - x_2(t)x_7(t)$, $x_8^{(2)}(t) = -(x_8^{(1)}(t))^2$. The noisy data are computed via $y_{ji} = x_j(t_i) + \epsilon_{ji}$, for $i = 1, \dots, n$ and $j = 1, \dots, 8$, with $t_i = i/n$ and ϵ_{ji} sampled independently from $N(0, \sigma^2)$. We consider various noise levels: $\sigma = 0.2, 0.5, 0.8$, and various sample sizes: $n = 100, 200, 500$.

Table 1: Simulation Design 1

(a) Metric M_1				(b) Metric M_3			
	$d = 10$	$d = 100$	$d = 1000$		$d = 10$	$d = 100$	$d = 1000$
$n = 100$	0.314	0.345	0.646	$n = 100$	1.027	2.191	6.740
$n = 200$	0.196	0.188	0.209	$n = 200$	0.631	1.014	1.779
$n = 500$	0.109	0.116	0.112	$n = 500$	0.320	0.638	0.892

(c) Metric M_2				(d) Metric M_4			
	$d = 10$	$d = 100$	$d = 1000$		$d = 10$	$d = 100$	$d = 1000$
$n = 100$	0.404	0.478	0.844	$n = 100$	1.132	2.342	7.203
$n = 200$	0.212	0.223	0.264	$n = 200$	0.686	1.034	1.834
$n = 500$	0.124	0.146	0.160	$n = 500$	0.343	0.643	0.947

Table 2: Simulation Design 2

(a) Metric M_1				(b) Metric M_3			
	$\sigma = 0.2$	$\sigma = 0.5$	$\sigma = 0.8$		$\sigma = 0.2$	$\sigma = 0.5$	$\sigma = 0.8$
$n = 100$	0.041	0.067	0.119	$n = 100$	0.182	0.243	0.412
$n = 200$	0.037	0.047	0.077	$n = 200$	0.172	0.190	0.262
$n = 500$	0.030	0.037	0.046	$n = 500$	0.159	0.173	0.192

(c) Metric M_2				(d) Metric M_4			
	$\sigma = 0.2$	$\sigma = 0.5$	$\sigma = 0.8$		$\sigma = 0.2$	$\sigma = 0.5$	$\sigma = 0.8$
$n = 100$	0.053	0.103	0.165	$n = 100$	0.194	0.329	0.541
$n = 200$	0.047	0.084	0.113	$n = 200$	0.179	0.268	0.360
$n = 500$	0.042	0.072	0.083	$n = 500$	0.177	0.228	0.260

4.2 Simulation results

In each simulation design, we employ four metrics to evaluate the performance of the proposed two-stage estimator:

$$\begin{aligned} M_1 &= \int_0^1 \left\| \widehat{\mathbf{f}}(\mathbf{x}(t), \mathbf{x}^{(1)}(t), \dots, \mathbf{x}^{(\nu-1)}(t)) - \mathbf{f}_0(\mathbf{x}(t), \dots, \mathbf{x}^{(\nu-1)}(t)) \right\|_2 dt, \\ M_2 &= \int_0^1 \left\| \widehat{\mathbf{f}}(\widehat{\mathbf{x}}(t), \widehat{\mathbf{x}}^{(1)}(t), \dots, \widehat{\mathbf{x}}^{(\nu-1)}(t)) - \mathbf{f}_0(\mathbf{x}(t), \dots, \mathbf{x}^{(\nu-1)}(t)) \right\|_2 dt, \\ M_3 &= \max_{j=1,\dots,d} \int_0^1 \left| \widehat{f}_j(\mathbf{x}(t), \mathbf{x}^{(1)}(t), \dots, \mathbf{x}^{(\nu-1)}(t)) - f_{0,j}(\mathbf{x}(t), \dots, \mathbf{x}^{(\nu-1)}(t)) \right| dt, \text{ and} \\ M_4 &= \max_{j=1,\dots,d} \int_0^1 \left| \widehat{f}_j(\widehat{\mathbf{x}}(t), \widehat{\mathbf{x}}^{(1)}(t), \dots, \widehat{\mathbf{x}}^{(\nu-1)}(t)) - f_{0,j}(\mathbf{x}(t), \dots, \mathbf{x}^{(\nu-1)}(t)) \right| dt. \end{aligned}$$

Metrics M_1 and M_3 measure the differences between the target and the second-stage deep neural network estimator in the L_2 norm and in the max norm, respectively, while M_2 and M_4 gauge the overall performance of the proposed two-stage estimator in these two norms respectively. A total of 100 independent replications are run for each design and the results are summarized in Tables 1 and 2.

As expected, the deviations measured by M_2 (M_4) are greater than those by M_1 (M_3) unanimously. Our results further show that the accuracy of the estimator diminishes as the dimension of the ODE grows and/or the noise-to-signal ratio increases. Moreover, a larger sample size yields a smaller deviation across all cases, which is in line with the theoretical results.

5 Real Data Analysis

In this section, we illustrate an application of our method to the Covid-19 infection cases. The data are downloaded from *New York Times*. (2021) <https://github.com/nytimes/covid-19-data>. This dataset contains daily new COVID-19 cases reported in individual states across the United States during 03/23/2020–05/07/2021, with 411 observations for each state. As an example, the orange curves in the four panels of Figure 1 display the number of the recorded daily new cases in four states, respectively: California, Texas, New York, and Florida.

Here, we attempt to use a system of ODEs to characterize the rate of changes of new cases over the 50 states *simultaneously*. Specifically, we consider a 50-dimensional second-order ODE system, as in (1) with $\mathbf{x}(t) = (x_1(t), \dots, x_{50}(t))^\top$ representing the number of Covid-19 infection cases at time t . With the daily new cases, we first calculate the accumulated daily cases for each state, i.e., y_{ji} in (3). We then apply the proposed two-stage estimation approach to estimate the function \mathbf{f}_0 . The filtered daily new cases are shown as blue curves in Figure 1 for the four selected states, while the deep neural network estimator $\widehat{\mathbf{f}}_0$ is shown in green. The results demonstrate the effectiveness and foreseeability of our method: when the estimated growth rate reaches the highest value, the daily new cases will peak roughly one month later.

To further illustrate the strength of our approach, we compare the proposed method with the traditional nonparametric estimation of the derivative of the regression function that estimates the growth rate of each state separately. The top two panels in Figure 2 show the growth rates that are estimated separately for three states in the western (Utah, Nevada, and Idaho) and northeastern (Connecticut, Rhode Island, and Massachusetts) U.S., respectively. The growth rates estimated using our methods are depicted in the bottom two panels. It is apparent that the estimates based on the two methods are quite different, and our estimates are more consistent with what is expected: geographically adjacent states should have strong interactions and hence share similar growth rates. This further shows the superiority of our method, in that it effectively incorporates the interactive processes among the neighboring states.

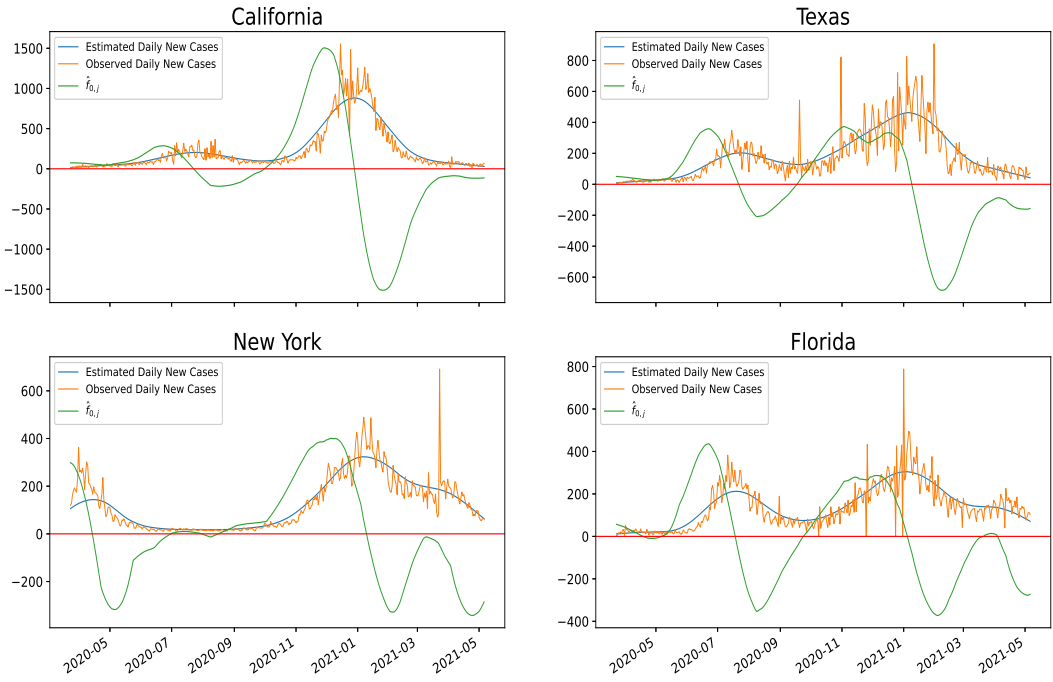


Figure 1: Green curve is the estimated growth rate for California, Texas, New York State and Texas. Blue Curve is the estimated daily new cases and yellow curve is the observed daily new cases.

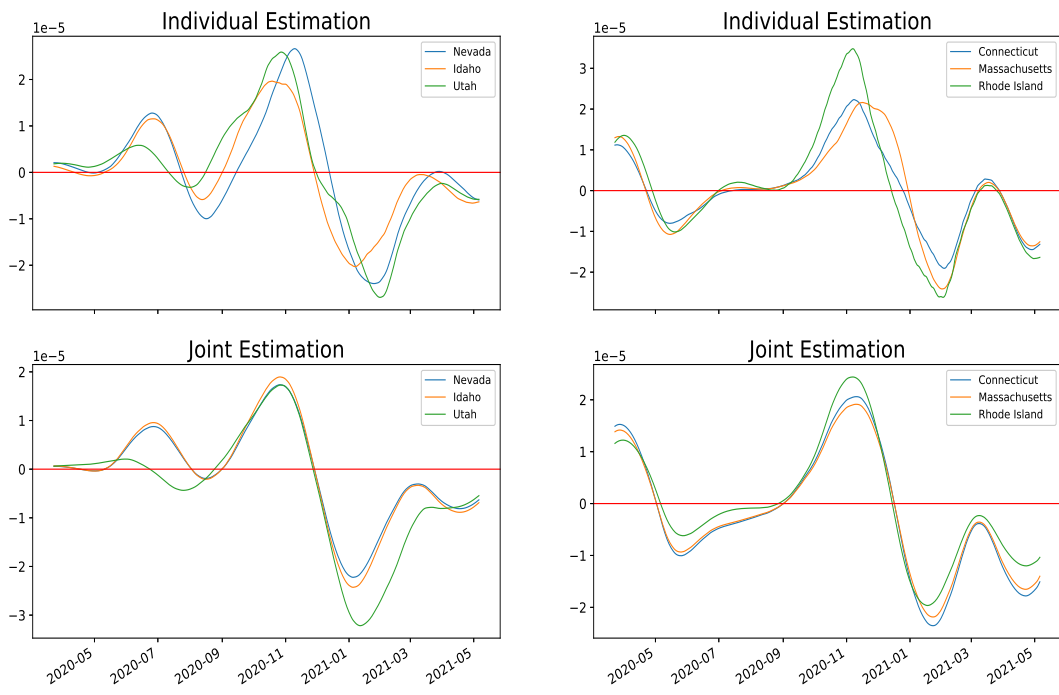


Figure 2: Comparison between individual estimation and joint estimation (the growth rates are standardized by population size). Top two panels: estimate individually. Bottom two panels: estimate jointly after calibrating using deep neural network. Left two panels: Western States. Right two panels: Eastern States.

References

[Bauer and Kohler, 2019] Bauer, B. and Kohler, M. (2019). On deep learning as a remedy for the curse of dimensionality in nonparametric regression. *Ann. Statist.*, 47(4):2261–2285.

[Benson, 1979] Benson, M. (1979). Parameter fitting in dynamic models. *Ecological Modelling*, 6(2):97 – 115.

[Bhaumik and Ghosal, 2015] Bhaumik, P. and Ghosal, S. (2015). Bayesian two-step estimation in differential equation models. *Electron. J. Statist.*, 9(2):3124–3154.

[Biegler et al., 1986] Biegler, L. T., Damiano, J. J., and Blau, G. E. (1986). Nonlinear parameter estimation: A case study comparison. *AIChE Journal*, 32(1):29–45.

[Champion et al., 2019] Champion, K., Lusch, B., Kutz, J. N., and Brunton, S. L. (2019). Data-driven discovery of coordinates and governing equations. *Proceedings of the National Academy of Sciences*, 116(45):22445–22451.

[Chen et al., 2018] Chen, R. T. Q., Rubanova, Y., Bettencourt, J., and Duvenaud, D. K. (2018). Neural ordinary differential equations. In Bengio, S., Wallach, H., Larochelle, H., Grauman, K., Cesa-Bianchi, N., and Garnett, R., editors, *Advances in Neural Information Processing Systems*, volume 31, pages 6571–6583. Curran Associates, Inc.

[Chen et al., 2017] Chen, S., Shojaie, A., and Witten, D. M. (2017). Network reconstruction from high-dimensional ordinary differential equations. *Journal of the American Statistical Association*, 112(520):1697–1707. PMID: 29618851.

[Elbrächter et al., 2021] Elbrächter, D., Perekrestenko, D., Grohs, P., and Bölcskei, H. (2021). Deep neural network approximation theory. *IEEE Transactions on Information Theory*, 67(5):2581–2623.

[Farrell et al., 2021] Farrell, M. H., Liang, T., and Misra, S. (2021). Deep neural networks for estimation and inference. *Econometrica*, 89(1):181–213.

[Ferraty and Vieu, 2006] Ferraty, F. and Vieu, P. (2006). *Nonparametric functional data analysis: theory and practice*. Springer Science & Business Media.

[Gasser and Müller, 1984] Gasser, T. and Müller, H.-G. (1984). Estimating regression functions and their derivatives by the kernel method. *Scandinavian Journal of Statistics*, 11(3):171–185.

[Gasser et al., 1985] Gasser, T., Müller, H.-G., and Mammitzsch, V. (1985). Kernels for nonparametric curve estimation. *Journal of the Royal Statistical Society. Series B (Methodological)*, 47(2):238–252.

[Hall and Ma, 2014] Hall, P. and Ma, Y. (2014). Quick and easy one-step parameter estimation in differential equations. *Journal of the Royal Statistical Society: Series B (Statistical Methodology)*, 76(4):735–748.

[Hammer, 2000] Hammer, B. (2000). On the approximation capability of recurrent neural networks. *Neurocomputing*, 31(1):107 – 123.

[He et al., 2016] He, K., Zhang, X., Ren, S., and Sun, J. (2016). Deep residual learning for image recognition. In *2016 IEEE Conference on Computer Vision and Pattern Recognition (CVPR)*, pages 770–778.

[Henderson and Michailidis, 2014] Henderson, J. and Michailidis, G. (2014). Network reconstruction using nonparametric additive ode models. *PLOS ONE*, 9(4):1–15.

[Henderson and Loreau, 2019] Henderson, K. and Loreau, M. (2019). An ecological theory of changing human population dynamics. *People and Nature*, 1(1):31–43.

[Kobyzev et al., 2020] Kobyzev, I., Prince, S., and Brubaker, M. (2020). Normalizing flows: An introduction and review of current methods. *IEEE Transactions on Pattern Analysis and Machine Intelligence*, pages 1–1.

[Kohler and Langer, 2019] Kohler, M. and Langer, S. (2019). On the rate of convergence of fully connected very deep neural network regression estimates. *arXiv e-prints*, page arXiv:1908.11133.

[Li et al., 2019] Li, Q., Lin, T., and Shen, Z. (2019). Deep learning via dynamical systems: An approximation perspective. *ArXiv*, abs/1912.10382.

[Li et al., 2020] Li, Z., Han, J., E, W., and Li, Q. (2020). On the Curse of Memory in Recurrent Neural Networks: Approximation and Optimization Analysis. *arXiv e-prints*, page arXiv:2009.07799.

[Liang and Wu, 2008] Liang, H. and Wu, H. (2008). Parameter estimation for differential equation models using a framework of measurement error in regression models. *Journal of the American Statistical Association*, 103(484):1570–1583. PMID: 19956350.

[Liu et al., 2019] Liu, R., Boukai, B., and Shang, Z. (2019). Optimal Nonparametric Inference via Deep Neural Network. *arXiv e-prints*, page arXiv:1902.01687.

[Liu et al., 2020] Liu, R., Shang, Z., and Cheng, G. (2020). On Deep Instrumental Variables Estimate. *arXiv e-prints*, page arXiv:2004.14954.

[Lu et al., 2020] Lu, J., Shen, Z., Yang, H., and Zhang, S. (2020). Deep Network Approximation for Smooth Functions. *arXiv e-prints*, page arXiv:2001.03040.

[Lu et al., 2011] Lu, T., Liang, H., Li, H., and Wu, H. (2011). High-dimensional odes coupled with mixed-effects modeling techniques for dynamic gene regulatory network identification. *Journal of the American Statistical Association*, 106(496):1242–1258. PMID: 23204614.

[Lusch et al., 2018] Lusch, B., Kutz, J., and Brunton, S. (2018). Deep learning for universal linear embeddings of nonlinear dynamics. *Nat Commun*, 9, 4950.

[Paul et al., 2016] Paul, D., Peng, J., and Burman, P. (2016). Nonparametric estimation of dynamics of monotone trajectories. *The Annals of Statistics*, 44(6):2401–2432.

[Priestley and Chao, 1972] Priestley, M. B. and Chao, M. (1972). Non-parametric function fitting. *Journal of the Royal Statistical Society: Series B (Methodological)*, 34(3):385–392.

[Schmidt-Hieber, 2020] Schmidt-Hieber, J. (2020). Nonparametric regression using deep neural networks with relu activation function. *Ann. Statist.*, 48(4):1875–1897.

[Stone, 1985] Stone, C. J. (1985). Additive regression and other nonparametric models. *The annals of Statistics*, pages 689–705.

[Sun et al., 2020] Sun, M., Zeng, D., and Wang, Y. (2020). Modelling temporal biomarkers with semiparametric nonlinear dynamical systems. *Biometrika*, 108(1):199–214.

[Talwar and Namachchivaya Sri, 1992] Talwar, S. and Namachchivaya Sri, N. (1992). Control of chaotic systems: Application to the lorenz equations. In *Nonlinear Vibrations*, American Society of Mechanical Engineers, Design Engineering Division (Publication) DE, pages 47–58. Publ by ASME. Winter Annual Meeting of the American Society of Mechanical Engineers ; Conference date: 08-11-1992 Through 13-11-1992.

[Wang et al., 2020] Wang, S., Cao, G., and Shang, Z. (2020). Estimation of the Mean Function of Functional Data via Deep Neural Networks. *arXiv e-prints*, page arXiv:2012.04573.

[Weinan, 2017] Weinan, W. (2017). A proposal on machine learning via dynamical systems. *Communications in Mathematics and Statistics*, 5(1).

[Wu et al., 2019] Wu, L., Qiu, X., xiang Yuan, Y., and Wu, H. (2019). Parameter estimation and variable selection for big systems of linear ordinary differential equations: A matrix-based approach. *Journal of the American Statistical Association*, 114(526):657–667.